ORIGINAL PAPER

Iodine/iodide-doped polymeric nanospheres for simultaneous voltammetric detection of p-aminophenol, phenol, and p-nitrophenol

Sabereh Narouie[1] · Gholam Hossein Rounaghi[1] · Hamideh Saravani[2] · Mehdi Shahbakhsh[3]

Abstract

A sensor was developed for the first time based on polydopamine nanospheres doped with I_2, I^-, and IO_3^- species (PDA-Iodine), to determine the concentration of p-aminophenol (p-AP), phenol (Ph), and p-nitrophenol (p-NP) simultaneously. These polymeric nanospheres were successfully characterized using a variety of techniques including field emission scanning electron microscopy, transmission electron microscopy, X-ray photoelectron spectroscopy, Fourier transform infrared, Raman spectroscopy, and X-ray diffraction analysis. A carbon paste electrode was modified with the PDA-Iodine (CPE/PDA-Iodine). Because of the electrocatalytic activity of DA/DQ, I_2 and I^- species (in the structure of PDA-Iodine), CPE/PDA-Iodine shows enhancement in the electrooxidation peak currents as well as slight negative shift in peak potentials of p-AP, Ph, and p-NP compared with a bare carbon paste electrode. Under optimal experimental conditions, the linear calibration plots are linear in the ranges 0.5–120 µM for p-AP, 0.7–120 µM for Ph, and 1.0–100 µM for p-NP with limits of detection of 30, 40, and 80 nM for p-AP, Ph, and p-NP, respectively (S/N = 3). To prove the performance of the method, the repeatability of the signals of CPE/PDA-Iodine was evaluated and the RSD values obtained were 2.9%, 3.2%, and 3.1% for p-AP (45 µM), Ph (40 µM), and p-NP (40 µM), respectively. The CPE/PDA-Iodine is a promising new sensor for sensing p-AP, Ph, and p-NP simultaneously in tap and river water sample and the values of recoveries for spiked samples were in the range 94.0–104.4%.

Keywords p-Aminophenol · Phenol · p-Nitrophenol · Polydopamine-iodine nanospheres · Electrochemical sensor · Voltammetry

Introduction

Among the catecholamines, dopamine (DA) has attracted a remarkable attention during the past few years because of its wide applications in various fields such as bioimaging and adsorption due to the presence of active functional groups (such as amino, catechol, and some other groups) in its structure [1]. In 2007,

✉ Gholam Hossein Rounaghi
ronaghi@ferdowsi.um.ac.ir; ghrounaghi@yahoo.com

1 Department of Chemistry, Faculty of Sciences, Ferdowsi University of Mashhad, P.O. Box 9177948974, Mashhad, Iran

2 Inorganic Chemistry Research Laboratory, Department of Chemistry, University of Sistan and Baluchestan, P.O. Box 98135-674, Zahedan, Iran

3 Analytical Chemistry Research Laboratory, Department of Chemistry, University of Sistan and Baluchestan, P.O. Box 98135-674, Zahedan, Iran

Lee et al. first found out that the DA molecules can be oxidized and self-polymerized to form polydopamine (PDA) in a facile and simple process under mild conditions [2]. Recently, several researches have revealed that the PDA coatings are formed by combining covalent polymerization and noncovalent self-assembly [3]. However, there are disputes over its actual structure and polymerization mechanism, and they have not been clearly known yet.

Oxidation of catechol groups can only be formed under a basic condition, and the reaction can also proceed under neutral and acidic conditions in the presence of different oxidants like ammonium persulfate, potassium chlorate, and sodium periodate [4]. For example, the oxidation of catecholamines to the corresponding substituted benzoquinones has been studied for aqueous acidic perchlorate media (pH < 1), and the oxidizing agent is an aquametal ion (Tl^{III}, Mn^{III}, V^v, Co^{III}) [5]. It has been discovered that employing the oxidizing agent improves the polymerization of PDA molecules under the basic conditions (pH 8.5) significantly and

it results in the production of PDA under neutral or acidic conditions [6].

In this work, periodic acid was used as an oxidizing agent for oxidation of DA molecules through oxidative polymerization process [4] with a fast kinetic characteristic and it also leads to the formation of polydopamine nanospheres.

Phenolic compounds are well known as an important class of raw chemicals, which are extensively applied in many manufacturing industries such as producing plastics, petroleum, paper, dyes, drugs, and antioxidants [7]. The existence of phenolic compounds in water can be related to the degradation of plants and animal wastes as well as anthropogenic sources like industrial, domestic, and agricultural activities [8]. However, the excessive use of these compounds may cause serious environmental problems such as ecological risks and human health threats because of their toxicity [7, 9].

For instance, the level of p-AP in pharmaceutical formulations has been restricted to 50 ppm (detection limit of 23 μM) by the US [10], European [11], and Chinese Pharmacopoeias authorities. Phenol has been listed as a priority pollutant by the US Environmental Protection Agency (EPA) and the European Union (EU), and its lethal blood concentration has been determined as 0.15 mg/mL [12] assigned as the highest limit for phenol compounds and their derivatives in freshwater as 0.5 ppb and 0.1 ppb, respectively [13]. The highest permissible limit of exposure to p-NP in the aquatic environment was found to be 20 ppb (0.14 μM). Hence, because of these bad effects and high toxicity of p-NP, the US environmental agencies have classified it as one of the most toxic pollutants for living organisms and their surrounding environment [14]. Because of the toxicity of phenolic compounds, it is crucial to establish an efficient, trustworthy, selective, and sensitive method for simultaneous determination of the concentrations of p-AP, Ph, and p-NP, which are necessary for environmental protection, the treatment of safe water supplies, and human health. The conventional analytical methods applied for determination of p-AP, Ph, and p-NP simultaneously are spectrophotometry, [15] high-performance liquid chromatography [16], gas chromatography-mass spectrometry [17], liquid chromatography-tandem mass spectrometry [18], capillary electrophoresis [19], and fluorescence spectrometry [20]. However, due to their benefits of simple equipment, fast response, high accuracy, excellent sensitivity, and satisfactory selectivity, the electrochemical methods have attracted considerable attention. Hence, in this research, a new voltammetric sensor based on carbon paste electrode modified with iodine-iodide-doped polydopamine nanospheres (CPE/PDA-iodine) was reported for determination of the concentration of p-AP,

Ph, and p-NP in aqueous solutions. Ultimately, our fabricated sensor showed an excellent analytical performance for reliable simultaneous determination of these phenolic compounds in river water and tap water samples.
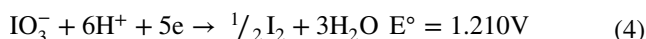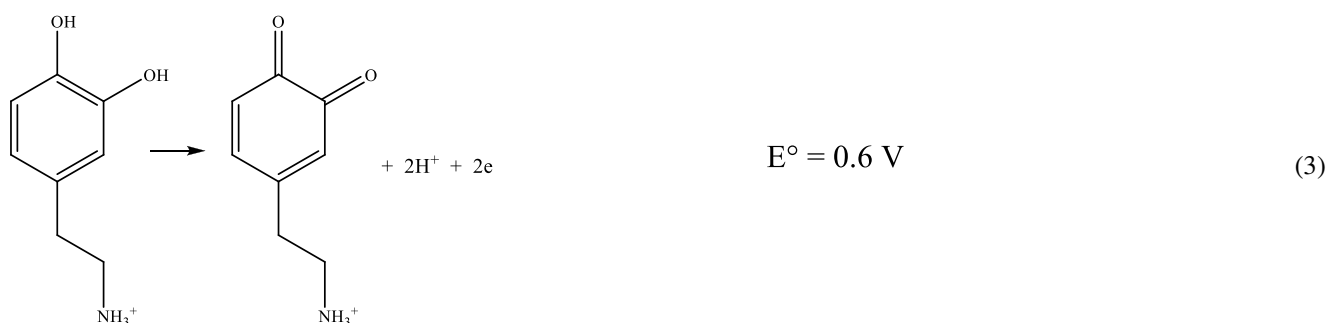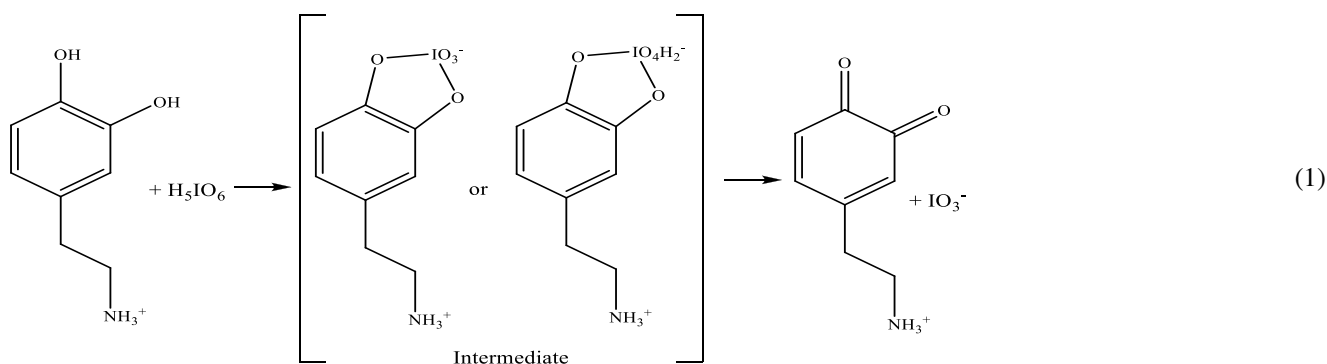
Experimental

Reagents and apparatus

Dopamine (DA), phenol (Ph), p-aminophenol (p-AP), p-nitrophenol (p-NP), periodic acid (H_5IO_6), paraffin oil (DC 350, density $= 0.88$ g cm^{-3}), graphite powder, sodium hydroxide, hydrochloric acid, and phosphoric acid of analytical grades ($> 99\%$) were purchased from Merck Chemical Company. The instrumentation data are given in S1.

Synthesis of PDA-Iodine

In a typical synthesis, 20 ml of an aqueous solution which contained 200 mg of DA (monomer precursor) and 200 mg of periodic acid (oxidizing agent) was mixed in a glass vial. Then, the color of the mixed solution was turned to brown immediately. After that, the mixture was stirred for 72 h, and the color of the solution changed to dark brown and became cloudy. The oxidation process of the hydroxyl functional groups in the DA structure was done by periodic acid. Ultimately, the reaction mixture was centrifuged and filtered, and the precipitate product was washed several times with deionized (DI) water (Millipore, 18.2 MΩ cm) followed by air drying for 48 h.

Results and discussion

The oxidation mechanisms of some catecholamines like adrenalin, ʟ-dopa, and dopamine with periodic acid are reported by Pelizzetti et al. At pH < 3, the catecholamines are converted to the open-chain o-benzoquinone, and in the pH range from 4 to 8, aminochrome is formed in solution [5]. Apart from that, Jaramillo et al. used sodium periodate (NaIO$_4$) as an oxidizing agent for oxidation of DA molecules in acidic media [21]. Similarly, Ponzio et al. reported the oxidation of dopamine with various oxidants like ammonium copper sulfate, sodium periodate, and also peroxodisulfate, and proving that the sodium periodate can be used as an oxidizing agent for the fast and homogeneous deposition of PDA films with exceptional properties [22]. Thus, herein, we used periodic acid for the oxidation of DA based on the following reaction (Eq. 1):

$$(1)$$

$$H_5IO_6 + H^+ + 2e \rightarrow IO_3^- + 3H_2O \quad E° = 1.567V \quad (2)$$

$$E° = 0.6 \text{ V} \quad (3)$$

$$IO_3^- + 6H^+ + 5e \rightarrow \tfrac{1}{2}I_2 + 3H_2O \quad E° = 1.210V \quad (4)$$

$$I_2 + 2e \rightarrow 2I^- \quad E° = 0.5355V \quad (5)$$

Hence, the final products are polydopamine nanospheres with adsorbed iodine which is present in PDA in the form of elemental iodine, iodide, and partially IO_3^- anions (the standard reduction potentials and related half reaction are given in Eqs. 2–5).

## Morphological and FT-IR characterization of PDA-Iodine

According to Fig. 1A–D, FESEM and TEM analyses were employed to characterize the morphology of the obtained PDA-Iodine nanospheres. FESEM images show regular spheres with diameters in the range 80–480 nm. In addition, the PDA-Iodine nanospheres have solid structures, confirmed by TEM characterization. FT-IR analysis discussed in S4 and Fig. S1 shows the presence of C=C, C=N, C=O, and OH vibrations indicating the polymerization of dopamine.

XPS characterization

Full-range XPS spectra were provided for further investigation of the chemical structure of PDA-Iodine and determination of the oxidation state of the adsorbed iodine on polydopamine surface. In Fig. 2, the XPS survey spectrum shows the peaks related to C 1 s, N 1 s, O 1 s, and I 3d in the PDA-Iodine structure. The binding energy of C 1 s was found at 285 eV, the N 1 s at 400 eV, the O 1 s at 532 eV, and the I 3d twinning at 621 and 632 eV.

Figure 2B shows a detailed analysis of the C 1 s peak for PDA-Iodine. The high resolution of C 1 s core-level spectrum can be deconvoluted into three different peaks: C–C/C–H (285.19 eV); C–O/C–N (286.57 eV); C = O (288 eV) [23]. The presence of catechol and quinone groups in polydopamine nanospheres is confirmed by C–O and C = O binding energies [24]. As shown in Fig. 2C, in the spectra of PDA nanospheres, two N 1 s peaks appeared which are related to the components of –NH (399.28 eV) and –NH₂ (400.61 eV), respectively. As shown in Fig. 2D, the O 1 s core-level spectrum can be deconvoluted

Fig. 1 FESEM images of PDA-Iodine (**A**, **B**) and TEM images of PDA-Iodine (**C**, **D**)
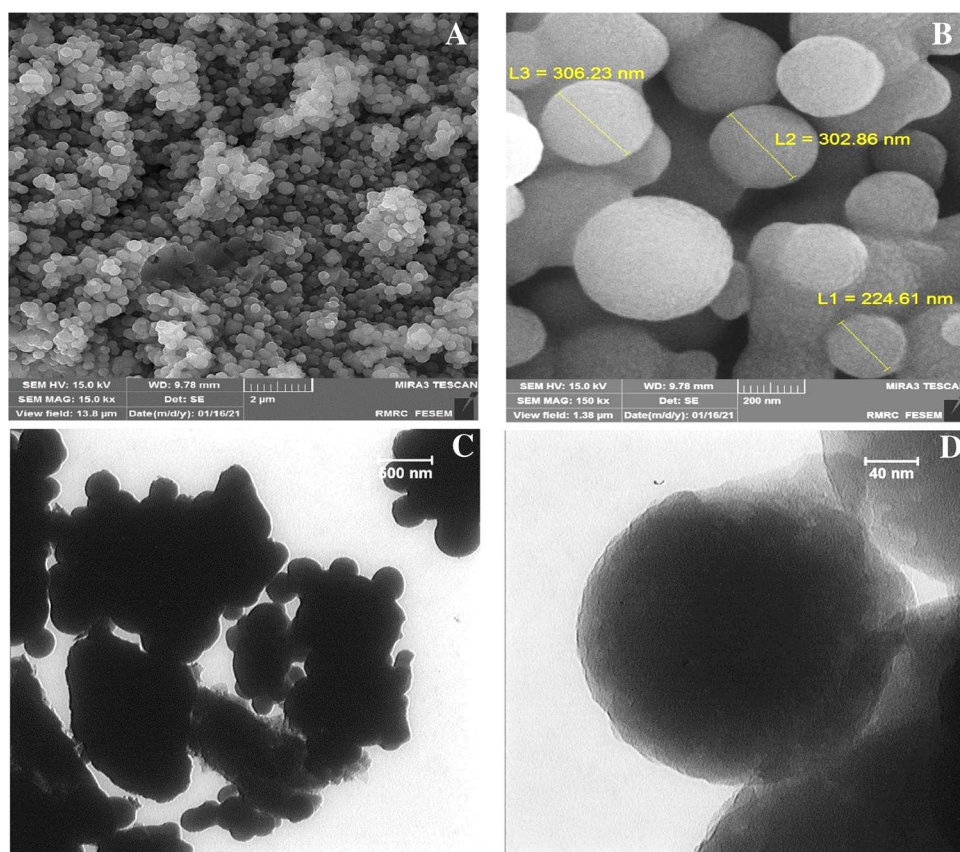
into two typical peaks: O = C (531.64 eV) and O–C (532.71 eV), which are related to quinone and catechol form of dopamine [25]. In addition, the binding energy at 532.70 eV is related to the adsorbed or integrated water molecules and other oxygen-containing species [26]. The high-resolution spectrum of I 3d is shown in Fig. 2E, in order to assess the chemical environment of iodine. The previous reports stated that the I 3d twinning peaks at 621.00 and 632.00 eV could be assigned to the multitude of chemical bonds, including elemental iodine, iodide, and polyiodide anions (I_3^- and I_5^-), but in the Raman spectra of PDA-Iodine, as seen in Fig. S2A, no Raman bands typical for I_3^- (109 cm^{-1}) or I_5^- (167 cm^{-1}) are registered [27] and the only one peak in 209 cm^{-1} is assigned to the iodine species [28]. As shown in Fig. 2E, two major peaks appeared at 619.17 eV and 630.38 eV due to the spin–orbit splitting resulting in 3d5/2 and 3d3/2 peaks, indicating that the iodine is adsorbed in the PDA nanospheres. In addition, two strong peaks

at 620.53 and 632.01 eV are observed, which can be related to the chemical bonding between nitrogen ion and iodide [27, 29, 30]. Furthermore, there are two small peaks at 623.60 and 634.85 eV, which are related to the iodate ion [30].

The powder X-ray diffraction pattern of PDA-Iodine shows a wide and blunt peak, representing an amorphous nature (Fig. S2B). The probable structure of PDA-Iodine is shown in Scheme 1.

Electrochemical characterization of CPE/PDA-Iodine for simultaneous determination of the concentration of p-AP, Ph, and p-NP

More details about the sensor preparation and CV of CPE/PDA-Iodine in PBS (0.1 M, pH 2.0) are given in S3, S5, and Fig. S3. The electrochemical behaviors of p-AP, Ph, and p-NP at the surface of bare CPE (BCPE) and CPE/PDA-Iodine were studied in PBS (phosphate buffer solution, 0.1 M, pH 2.0). In Fig. 3, three broad

oxidation peaks with low intensity are noticed on the BCPE for p-AP, Ph, and p-NP at 0.52, 1.04, and 1.3 V, respectively, indicating that the molecules are clearly indistinguishable on the bare electrode. In comparison, the CPE/PDA-Iodine electrode shows three stronger oxidation peaks for p-AP, Ph, and p-NP molecules at 0.46, 1.01, and 1.23 V, respectively, illustrating the excellent electrocatalytic performance of CPE/PDA-Iodine electrode towards the redox reactions of each analyte which is present in solution. The great increase in the intensity of redox peaks shows that the PDA-Iodine has a fast electron transfer in the redox process compared to BCPE.

Electrocatalytic determination of p-AP, Ph, and p-NP at CPE/PDA-Iodine electrode

The ability of CPE/PDA-Iodine electrochemical sensor towards the electrocatalytic determination of p-AP, Ph, and p-NP was studied by taking advantage of the well-defined electrochemical signature. As illustrated in Fig. 4, the CPE/PDA-Iodine shows an excellent performance towards individual catalytic oxidation of p-AP, Ph, and p-NP molecules to their respective products in 0.1 M PBS (pH 2.0). The CPE/PDA-Iodine illustrates a couple of oxidation–reduction peaks at 0.27/0.17 V and also, a broad oxidation peak is seen which is centered at 0.65 V (from 0.44 to 0.84 V). The CV curves of CPE/PDA-Iodine in the presence of different concentrations of p-AP are shown in Fig. 4A. According to this figure, an anodic peak appeared at 0.47 V and a new reduction peak is noticed at 0.43 V, related to the reduced form of p-AP. With successive addition of p-AP, a gradual increase in the peak current of p-AP is also observed. A probable mechanism for the oxidation process of p-AP molecules is given in Eq. (6) [31].

Because of the presence of different redox species (DA, DQ, I_2, I^-, and I_3^-) on the electrode surface, it is very difficult to detect the actual mechanisms of interactions between the analytes and the modifier; however, the changes of the peak currents corresponding to the effects of electroactive species in the structure of the modifier with increasing of the concentration of analyte confirm the interaction between the analyte and the proposed modifier.

A similar experiment was carried out for the Ph. The electrocatalytic oxidation of Ph at the CPE/PDA-Iodine can be explained with the possible mechanism which is shown in Fig. 4B. During the CV scan, as soon as the phenol molecules reach potential of 1.0 V, they are oxidized electrochemically to phenosemiquinone radicals, and these intermediates selectively oxidize the Ph molecules to hydroquinone and catechol, while during the backward scan, the new reduction peaks corresponding to hydroquinone and catechol appear at potentials of 0.66 V and 0.57 V, respectively (Eq. (7)) [32, 33]. The same study was conducted for the p-NP. As shown in Fig. 4C, the anodic peak at 1.26 V corresponds to the oxidation of nitrophenol to the 4-nitrophenoxy radical (oxidation of hydroxyl group). This monoradical can experience a dimerization process. At negative potential, the p-NP molecule is reduced to p-aminophenol, but because this process takes place at potentials lower than the reduction potential window of the water molecules, therefore, the reduction peak cannot be observed. The peak current of p-NP at 1.3 V increases with an increase in the concentration of p-NP. The proposed mechanism is shown in Eq. (8) [34].

The electrooxidation peak currents of the iodine species (I_2/I^- and I^-/I_3^-) at the modified electrode decrease upon increase of the concentration of p-NP in solutions.

It seems that the presence of the aromatic benzene rings and the adsorbed iodine species on the nanospheres surfaces result in the accumulation (π-π interaction between aromatic rings of polymer and analytes and the interaction of the electron cloud of the iodine species and the analytes molecules) of the analytes on the electrode surface. In addition, since the p-nitrophenol molecule has a nitro group, it can cause a direct oxidation–reduction reaction with the iodine species which results in a decrease in the oxidation peak current of the iodine species, as is seen in Fig. 4C. Such evidences confirm the interactions between the iodine species or their oxidation intermediates or their oxidation products with p-NP molecules.
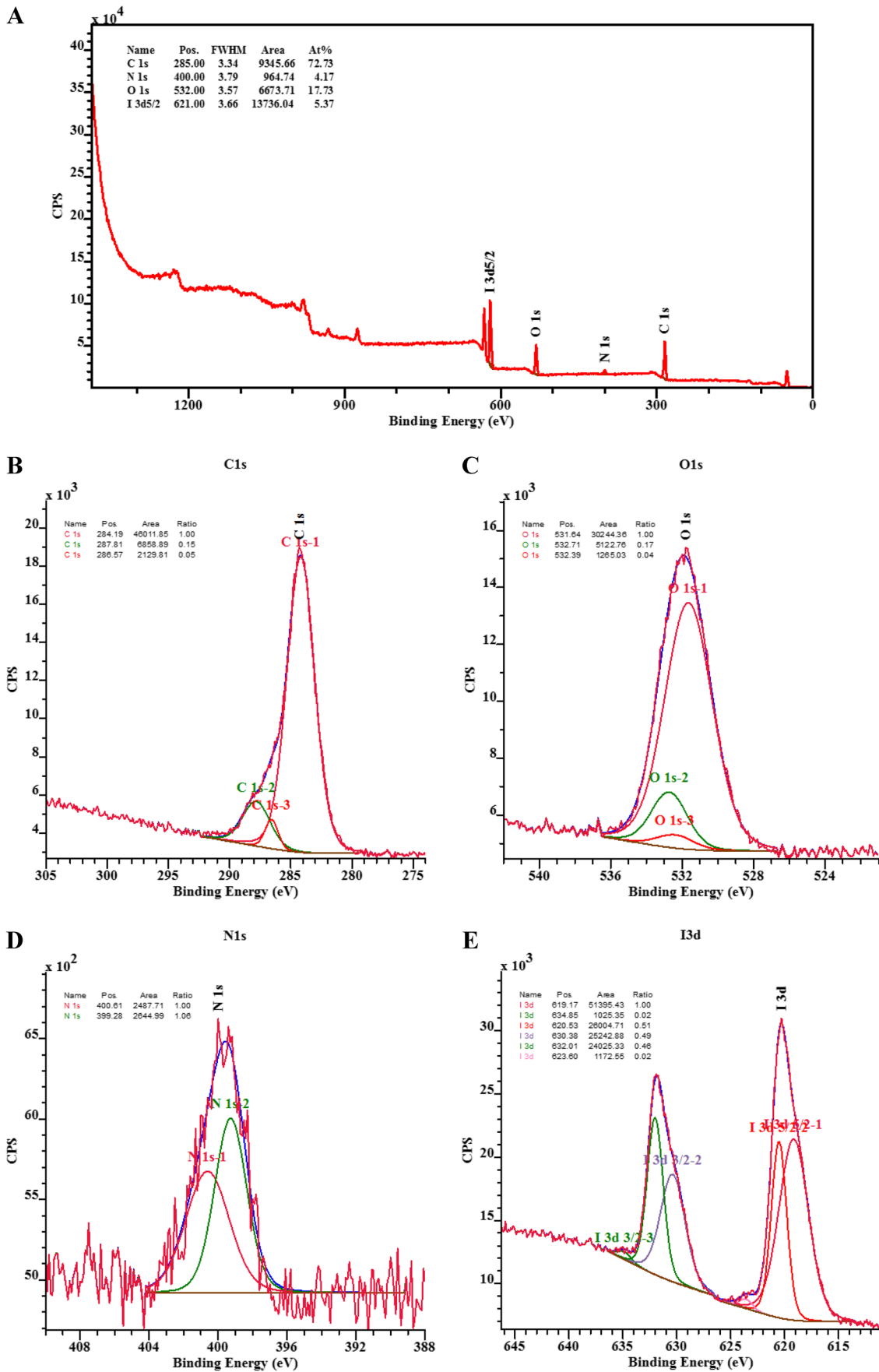
A

**B** C1s

C O1s

D N1s

E I3d

◄**Fig. 2** **A** XPS spectrum related to the elemental survey scan of PDA-Iodine. **B** Curve fitting of C 1 s XPS spectra. **C** Curve fitting of O 1 s XPS spectra. **D** Curve fitting of N 1 s XPS spectra. **E** Curve fitting of I 3d XPS spectra (All binding energy values were calibrated by fixing the C (1 s) core level to the 285.0 eV. XPS peaks were deconvoluted using the SDP software (version 4.1) with 80% Gaussian-20% Lorentzian peak fitting)

(8)

(6)
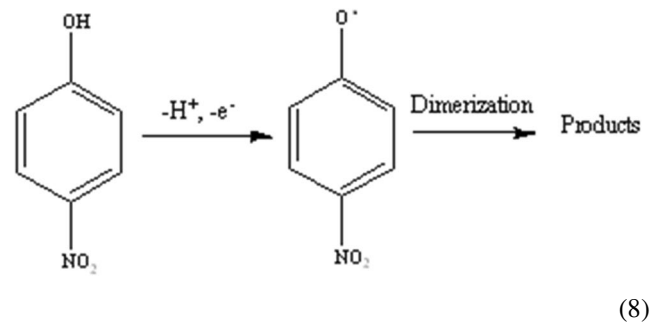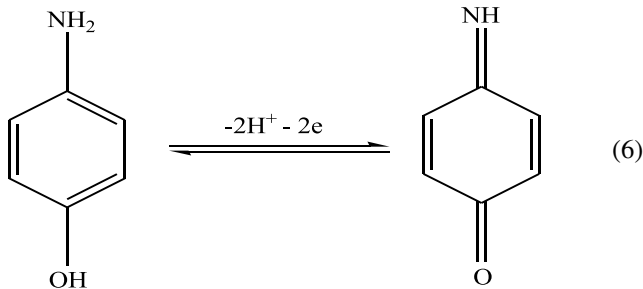
Simultaneous quantitative determination of p-AP, Ph, and p-NP using DPV

Optimization results (given in S6 and S7) reveal that the CPE/PDA-Iodine shows maximum peak currents and peak-to-peak separations at pH 2 and the electrochemical

(7)
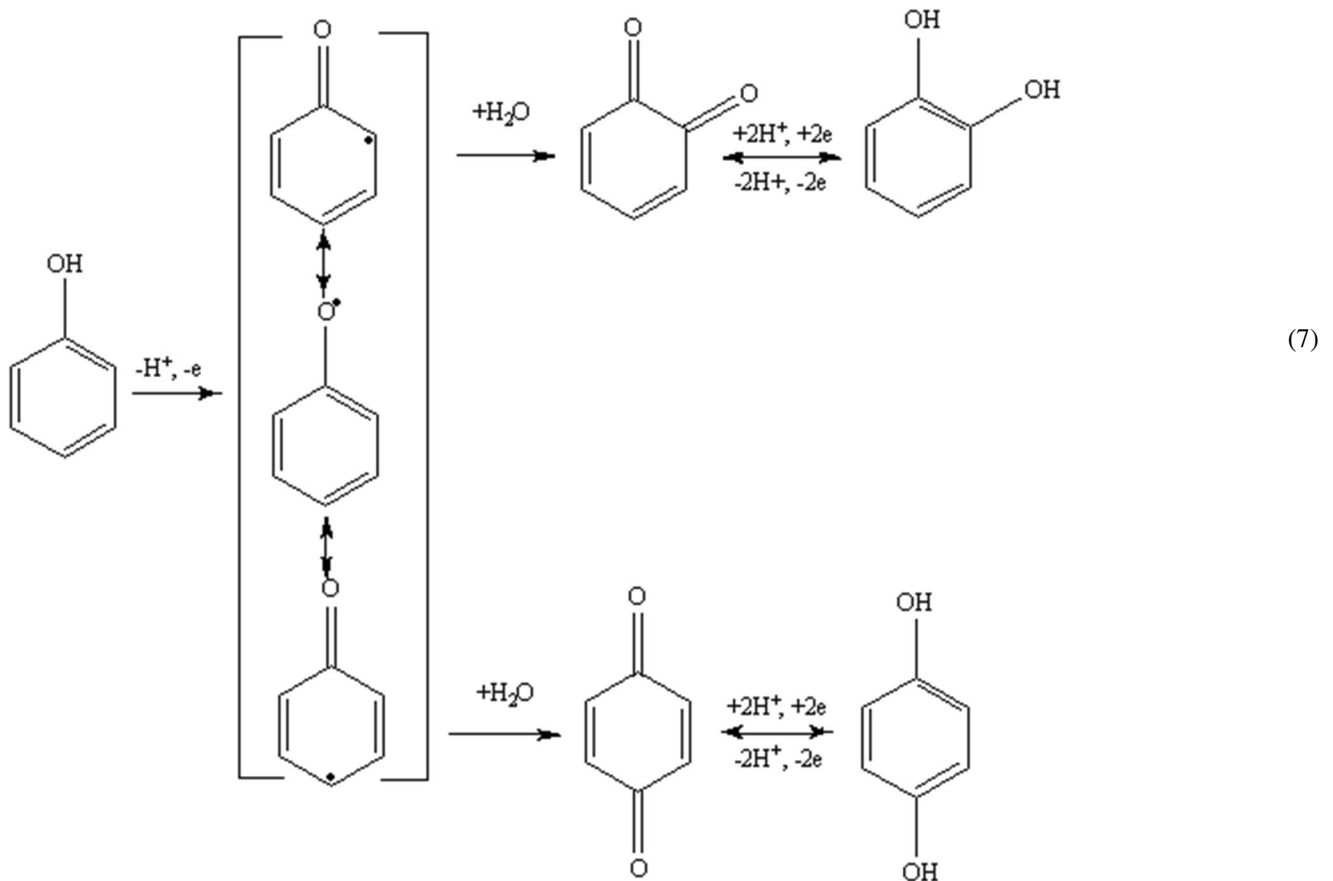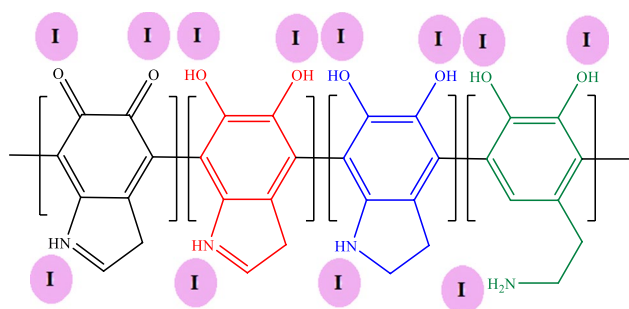
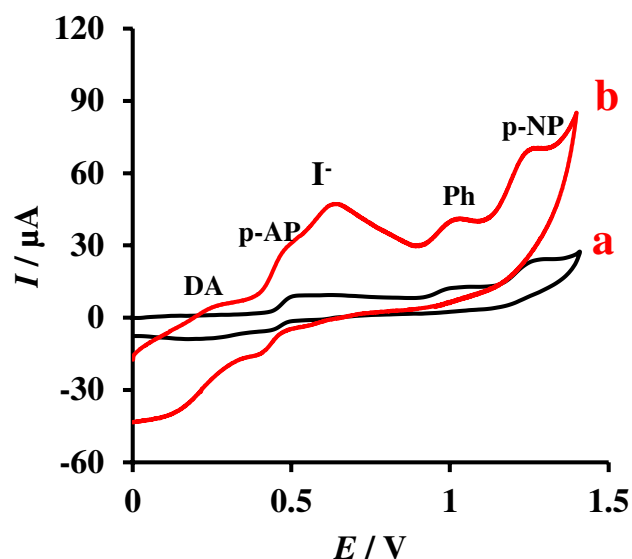**Scheme 1** Structure of polydopamine-Iodine

Fig. 3 CVs at (**a**) BCPE and (**b**) CPE/PDA-Iodine in 0.1 M PBS (pH 2.0) containing p-AP (80 µM), Ph (90 µM), and p-NP (70 µM)

reactions of p-AP, Ph, and p-NP molecules on the modified electrode are diffusion-controlled processes. However, differential pulse voltammetry (DPV) experiments were applied for simultaneous measurement of the concentration of p-AP, Ph, and p-NP in solutions under optimal experimental conditions using the fabricated electrochemical sensor. Figure 5 shows the DPV curves of p-AP, Ph, and p-NP molecules at their different concentrations. As depicted in this figure, the anodic peak currents increased linearly with an increase in the p-AP, Ph, and p-NP concentrations in solutions. The corresponding calibration plot for p-AP can be noticed in Fig. 5. The anodic peak currents of p-AP increase linearly with its concentration between 0.5 and 120 µM. The linear equation is expressed as: I (µA) = (0.1128 ± 0.0020) $[C_{p-AP}(µM)] + 1.2263 ± 0.1142$ with correlation coefficient of 0.9963 and the current sensitivity of 0.8978 µA.µM^{-1}. cm^{-2}. This figure also shows the related calibration plot for Ph. The anodic peak current also increases linearly

with the concentration of Ph between 0.7 and 120 µM. The linear equation is expressed as: I (µA) = (0.1161 ± 0.0022) $[C_{Ph}$ (µM)] + 1.6961 ± 0.1167 with correlation coefficient of 0.9961 and the current sensitivity of 0.9242 µA.µM^{-1}.cm^{-2}. Figure 5 also illustrates the related calibration plot for p-NP. The anodic peak currents increase linearly with the concentration of p-NP between 1.0 and 100 µM. The related linear equation is calculated as: I (µA) = (0.1611 ± 0.0034) $[C_{p-NP}$ (µM)] + 2.0328 ± 0.1870 with correlation coefficient of 0.9956 and the current sensitivity of 1.283 µA.µM^{-1}.cm^{-2}. Detection limits were calculated based on the relationship of LOD = 3Sblank/m where S blank is the relative standard deviation of blank signals ($n = 10$) and m is the slope of the calibration plot. Hence, LOD values were obtained as 30, 40, and 80 nM for p-AP, Ph, and p-NP, respectively. Moreover, based on the results given in S8 and Table S1, the proposed sensor is an excellent candidate for simultaneous quantitative determination of p-AP, Ph, and p-NP in solutions. Furthermore, as discussed in S9, S10, and Table S2, the proposed sensor shows excellent selectivity and stability indicating its applicability as a promising candidate for selective and stable detection of these three phenolic pollutants.

Application of CPE/PDA-Iodine electrochemical sensor for the quantitative determination of p-AP, Ph, and p-NP in real samples

In order to verify the analytical application of the proposed sensor, it was used for simultaneous measurement of the concentrations of p-AP, Ph, and p-NP in real samples, including tap water and river water samples. Tap water and river water samples were centrifuged (at 5000 rpm) to remove solid materials, and then the pH values of the samples were adjusted to 2, using 0.1 M PBS. Twenty-milliliter aliquots of these samples were transferred in electrochemical cell and the amount of analytes was determined through recording DPVs (by calculating the peak currents at 0.46 V for p-AP, 1.01 V for Ph, and 1.23 V for p-NP). The results show that the analyzed real samples do not contain these phenolic compounds at the LOD level. Therefore, the applicability of the proposed sensor for real sample analysis was tested through analysis of the spiked samples using the standard addition method. Therefore, appropriate amounts of the analytes (given in Table S3) were spiked into each samples (which their pH values were adjusted to 2, using 0.1 M PBS) to determine the recovery values using the proposed method. As depicted in Table S3. The values of the recoveries were in the range from 94.0 to 104.4%, which confirms that the matrix of the real samples does not cause any interference in determination of the concentrations of these phenolic compounds in aqueous solutions. In addition, the samples were also analyzed by HPLC for comparison.

Fig. 4 CVs at CPE/PDA-Iodine in 0.1 M PBS (pH 2.0) containing increasing concentrations of p-AP (**A**), Ph (**B**) (25, 50, 100 μM from inner to outer), and p-NP (**C**). (10, 20, 30, 40, 50, 60, 75, and 100 μM from inner to outer)
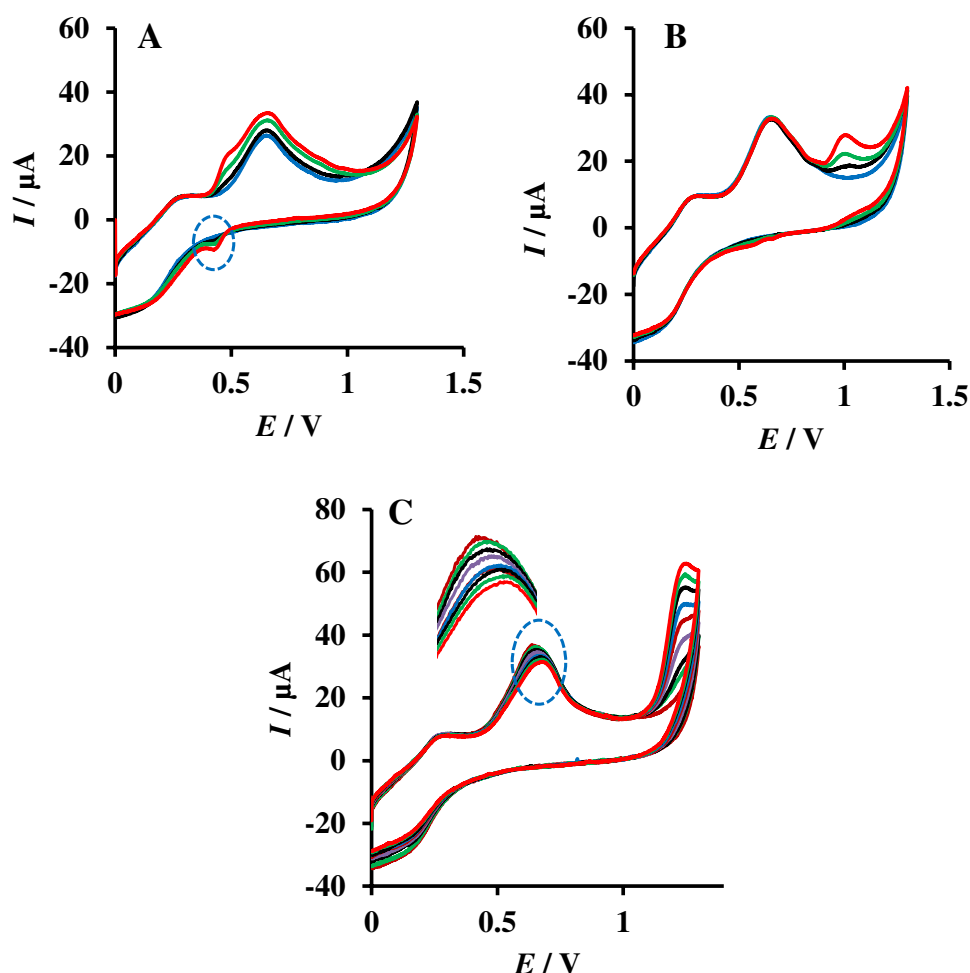

The representative HPLC chromatogram in Fig. S7 (HPLC conditions were given S2) shows the separation of p-AP (60 μM), Ph (80 μM), and p-NP (100 μM) in optimum experimental conditions. As can be seen in Table S3, the results obtained with the proposed method are in good agreement with those of standard HPLC method indicating the accuracy of the results. Therefore, the developed sensor gives a promising tool for the simultaneous determination of p-AP, Ph, and p-NP in tap and river water samples with desirable recoveries. It is important to note that like many solid electrodes, the electrode fouling due to accumulation of the oxidation products of analytes is a problem. Thus, when necessary, the electrode surface was regenerated by pushing the graphite paste out of the glass tube and polishing it by weighing paper.

Conclusion

Simultaneous quantitative determination of phenolic pollutants in water samples is an actual area of investigation in modern electroanalysis. The present work focuses on the preparation of a cheap, stable, selective, and sensitive sensor for simultaneous monitoring the concentration of three toxic phenolic pollutants—p-aminophenol (p-AP), phenol (Ph), and p-nitrophenol (p-NP)—in water samples. PDA-Iodine nanospheres were prepared and implemented to modify a carbon paste electrochemical sensor. The CPE/PDA-Iodine electrode was applied as a novel electrochemical sensor with well-defined oxidation peaks for the simultaneous quantitative determination of these phenolic compounds. The CPE/PDA-Iodine sensor showed an excellent electrocatalytic activity because of the presence of various redox species (DA/DQ, I_2/I^-) on the electrode surface. The proposed sensor has advantages like low detection limits, appreciable stability, good selectivity, acceptable repeatability, and cost-effectiveness for measurement of the concentration of these phenolic compounds. The maximum interfering effects were seen for dihydroxybenzene isomers, chlorophenols, and meta and ortho isomers of AP and NP (meta and ortho isomers of AP and NP in the determination of p-AP and p-NP, respectively). Hence, the concentrations of these compounds should not be more than the levels determined in Table S2. In addition, this proposed sensor can be tested

Fig. 5 DPVs of CPE/PDA-Iodine in 0.1 M PBS (pH 2.0) containing mixed concentration of p-AP, Ph, and p-NP. [p-AP]:0.5–120 μM, [Ph]: $0.7 - 120$ μM, [p-NP]: 1.0–100 μM. The insets show plots of anodic peak current vs. concentration of p-AP, Ph, and p-NP, respectively. The error bars represent the standard deviation of three parallel tests (relative standard deviation (%RSD) was found to be < 3% for $n = 3$)
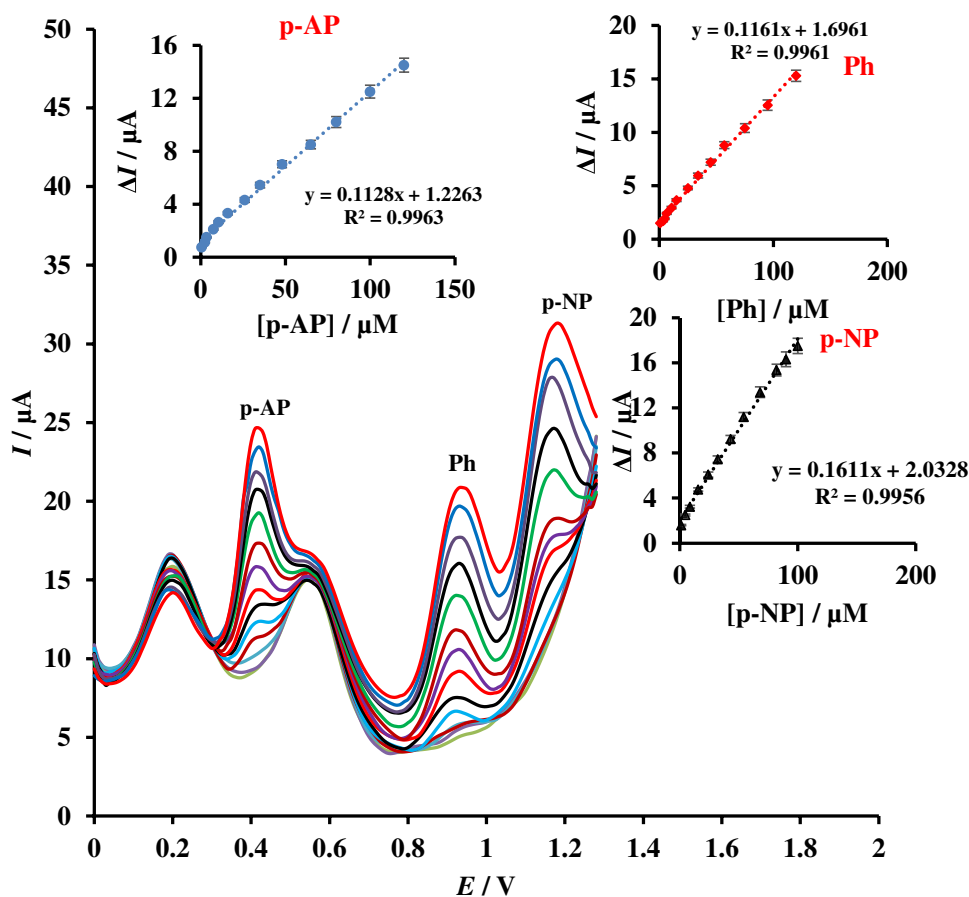
for determination of other phenolic pollutants (in water samples) or detection of pharmaceuticals in human blood and urine samples.

Declarations

Conflict of interest The authors declare no competing interests.

References

1. Jia S et al (2020) Polydopamine microsphere-incorporated electrospun fibers as novel adsorbents for dual-responsive adsorption of methylene blue. ACS Appl Mater Interfaces 12(44):49723–49736
2. Lee H et al (2007) Mussel-inspired surface chemistry for multifunctional coatings. Science 318(5849):426–430
3. Liu Y, Ai K, Lu L (2014) Polydopamine and its derivative materials: synthesis and promising applications in energy, environmental, and biomedical fields. Chem Rev 114(9):5057–5115
4. Yang J (2016) Mussel-inspired chemistry and its application. Wageningen University
5. Pelizzetti E, Mentasti E, Pramauro E (1976) Kinetics and mechanism of oxidation pathways of some catecholamines with periodic acid. J Chem Soc Perkin Trans 14:1651–1655
6. Lynge ME et al (2011) Polydopamine—a nature-inspired polymer coating for biomedical science. Nanoscale 3(12):4916–4928
7. Shen Y et al (2020) Defect-rich hexagonal boron nitride for the simultaneous determination of 4-aminophenol and phenol. Sens Actuators, B Chem 303:127248
8. Abu-Alsoud GF, Bottaro CS (2021) Porous thin-film molecularly imprinted polymer device for simultaneous determination of phenol, alkylphenol and chlorophenol compounds in water. Talanta 223:121727
9. Gan T et al (2017) Flexible graphene oxide− wrapped SnO2 hollow spheres with high electrochemical sensing performance in simultaneous determination of 4− aminophenol and 4− chlorophenol. Electrochim Acta 250:1–9
10. The United States Pharmacopeial Convention, The United States Pharmacopoeia 27-NF (The National Formulary), 2004. 2494
11. The European Pharmacopeial Convention, The sixth edition European Pharmacopoeia, The European Pharmacopeial Convention, 2007. 49
12. Kaffash A, Zare HR, Rostami K (2018) Highly sensitive biosensing of phenol based on the adsorption of the phenol enzymatic oxidation product on the surface of an electrochemically reduced graphene oxide-modified electrode. Anal Methods 10(23):2731–2739

13. Arfin T, Rangari SN (2018) Graphene oxide–ZnO nanocomposite modified electrode for the detection of phenol. Anal Methods 10(3):347–358
14. Hashemi SA et al (2020) Integrated polyaniline with graphene oxide-iron tungsten nitride nanoflakes as ultrasensitive electrochemical sensor for precise detection of 4-nitrophenol within aquatic media. J Electroanal Chem 873:114406
15. Filik H et al (2008) Development of an optical fibre reflectance sensor for p-aminophenol detection based on immobilised bis-8-hydroxyquinoline. Talanta 77(1):103–109
16. Escarpa A, Morales MAD, González MAC (2002) Analytical performance of commercially available and unavailable phenolic compounds using real samples by high-performance liquid chromatography–diode-array detection. Anal Chim Acta 460(1):61–72
17. Keser D et al (2020) Characterization of aroma and phenolic composition of carrot (Daucus carota 'Nantes') powders obtained from intermittent microwave drying using GC–MS and LC–MS/MS. Food Bioprod Process 119:350–359
18. Yazdinezhad SR et al (2013) Single-step extraction and cleanup of bisphenol A in soft drinks by hemimicellar magnetic solid phase extraction prior to liquid chromatography/tandem mass spectrometry. Anal Chim Acta 778:31–37
19. Xie T et al (2006) Simultaneous determination of positional isomers of benzenediols by capillary zone electrophoresis with square wave amperometric detection. J Chromatogr A 1109(2):317–321
20. Lu X et al (2017) Surface molecular imprinting on silica-coated CdTe quantum dots for selective and sensitive fluorescence detection of p-aminophenol in water. J Fluoresc 27(1):181–189
21 Jaramillo ASM, Barrera-Gutiérrez R, Cortes MT (2020) Synthesis, follow-up, and characterization of polydopamine-like coatings departing from micromolar dopamine-o-quinone precursor concentrations. ACS omega 5(25):15016–15027
22. Ponzio F et al (2016) Oxidant control of polydopamine surface chemistry in acids: a mechanism-based entry to superhydrophilic-superoleophobic coatings. Chem Mater 28(13):4697–4705
23. Rella S et al (2018) Investigation of polydopamine coatings by X-ray photoelectron spectroscopy as an effective tool for improving biomolecule conjugation. Appl Surf Sci 447:31–39
24. Wei Q et al (2010) Oxidant-induced dopamine polymerization for multifunctional coatings. Polym Chem 1(9):1430–1433
25. Zhang Q et al (2018) Distinguished Cr (VI) capture with rapid and superior capability using polydopamine microsphere: behavior and mechanism. J Hazard Mater 342:732–740
26. Barka-Bouaifel F et al (2011) Synthesis and photocatalytic activity of iodine-doped ZnO nanoflowers. J Mater Chem 21(29):10982–10989
27. Siuzdak K et al (2015) Enhanced photoelectrochemical and photocatalytic performance of iodine-doped titania nanotube arrays. RSC Adv 5(62):50379–50391
28. Eskola SM (1996) Kinetics of the toluene-iodine complex formation as revealed by Raman spectroscopy. Mol Phys 88(5):1205–1210
29. Yu F et al (2020) Synthesis of metal–organic framework nanocrystals immobilized with 3D flowerlike Cu–Bi-layered double hydroxides for iodine efficient removal. J Mater Res 35(3):299–311
30. Li K et al (2016) Combined DFT and XPS investigation of iodine anions adsorption on the sulfur terminated (001) chalcopyrite surface. Appl Surf Sci 390:412–421
31. de Souza JC, Zanoni MVB, Oliveira-Brett AM (2020) Genotoxic permanent hair dye precursors p-aminophenol and p-toluenediamine electrochemical oxidation mechanisms and evaluation in biological fluids. J Electroanal Chem 857:113509
32. Han C et al (2018) Selective electro-oxidation of phenol to benzoquinone/hydroquinone on polyaniline enhances capacitance and cycling stability of polyaniline electrodes. Chem Eng J 347:648–659
33. Narouie S et al (2022) Multiwalled carbon nanotubes/4, 4′-dihydroxybiphenyl nanolayered composite for voltammetric detection of phenol. Electroanalysis. 34:798–808
34. Narouie S, et al. (2021) Poly (Biphenol/biphenoquinone-vanadium (IV)) modified electrode as selective sensor for detection of 4-nitrophenol. Microchem J p. 106945